Small-angle X-ray scattering study of nanostructure evolution of β" precipitates in Al-Mg-Si alloy

C.-S. Tsao[1], U.-S. Jeng[2], C.-Y. Chen[1], T.-Y. Kuo[3]
[1]Nuclear Fuel and Materials Division, Institute of Nuclear Energy Research, Longtan, Taiwan
[2]National Synchrotron Radiation Research Center, Hsinchu 30076, Taiwan
[3]Department of Mechanical Engineering, Southern Taiwan University of Technology, Taiwan

Abstract

The *in-situ* synchrotron small-angle X-ray scattering and transmission electronic microscopy were employed to study the precipitation behavior of a naturally aged Al-Mg-Si alloy during artificial aging at 180℃. The nanostructural evolution of the rod-like β" precipitates with aging time is quantitatively and accurately determined from the SAXS analysis.

Keywords: Small-angle X-ray scattering; Aluminum alloys; Precipitation; Ageing

1. Introduction

Because of higher strength and lighter weight, aluminum alloys have been extensively used in the aerospace and automotive industries. The strengthening of Al-Mg-Si alloys mainly comes from the rod-like β" precipitates formed during the precipitation at artificially elevated temperature. Although numerous electronic transmission microscopy (TEM) investigations have been conducted on the nanostructural characterization and precipitation behavior of Al-Mg-Si alloys, the understanding [1-7] is still incomplete and a matter of controversy. Despite few differential scanning calorimetry (DSC) studies [6,8] could investigate effectively the evolution of the relative volume fraction of the precipitates, there is lack of systematic experiments on the temporal evolution of precipitate nanostructure and the corresponding precipitation kinetics. Moreover, the deleterious effect of natural aging on the subsequent artificial aging response of the Al-Mg-Si alloys is of increasing interest [1,8,9], and attributed to the clusters/Guinier-Preston (GP) zones formed during natural aging at room temperature (RT) and the subsequent dissolution of these cluster/ GP zones during the artificial aging [6,8,9]. Incorporating the Johnson-Mehl, Avrami, Kolmogorov (JMAK) kinetics into the DSC data measured for Al-Mg-Si alloy with natural aging effect, Esmaeili *et al*. [8] presented the only quantitative investigation on the kinetics of concurrent cluster dissolution and precipitation process during an artificial aging relevant to the yield strength of the alloys.

In the investigation of nanostructures evolution of a large number of particles in a bulk sample, the *in-situ* small-angle X-ray and neutron scattering (SAXS and SANS) are very powerful compared to the TEM technique. However, the SANS study for Al-Mg-Si alloy is very few, providing either the limited data [7] or too rough analysis [10] on the β" precipitates. Because the SAXS contrast between β" precipitates, MgSi, and matrix Al is very low, no SAXS study on the structural evolution of β" precipitates has been reported.

In this study, we perform SAXS for an Al-Mg-Si alloy with high flux and high-energy photons from synchrotron radiation. The penetration of 15 keV photons selected allows an optimum SAXS sample thickness of the alloys five folds thicker than that with 8 keV photons. Therefore, the scattering intensity from β" precipitates in the Al matrix can be further enhanced by the same factor, when the optimum sample thickness is used. The high flux together with the larger optimum sample thickness facilitates greatly the *in-situ* SAXS investigation for the precipitation behavior of the naturally aged Al-Mg-Si alloy during an artificial aging at 180

℃. With the *in-situ* SAXS result, we present temporal evolution of rod-like β" precipitates in the alloy, including radius, length and volume fraction of the precipitates. In addition, TEM is employed for the same specimen used in SAXS as a complementary tool to confirm the accuracy of our SAXS analysis. The precipitation kinetics with considering the natural aging effect, is established from this *in-situ* SAXS study.

2. Experiment

Al-Mg-Si alloy 6022 of 1mm in thickness was received from Alcoa Inc., USA. The composition of the alloy was (wt%): 0.58 Mg, 1.15 Si, 0.13 Fe, 0.06 Cu, 0.06 Mn. The sheet sample was solution treated at 560℃ for 40min and subsequently quenched into ice water. Afterwards, the alloy was naturally aged for 30 days at RT, in which period the clusters /GP zones were formed prior to the artificial aging for *in-situ* SAXS. The SAXS specimen cut from this sheet was prepared into 1cm×1cm area and an optimum thickness of 0.5mm. The *in-situ* SAXS measurement was carried out at the beam line BL01B of the National Synchrotron Radiation Research Center (NSRRC), Taiwan. The beamline delivers a photon flux of ~ 3×10^{11} photons/s in the energy range of 5-22 keV. The monochrome beam of 15 keV photons was collimated into 1 mm dia. by two pinholes separated at a distance of ~ 4.7 m, for our SAXS measurements. The specimen, fixed inside a small furnace with air-circulation cooling, was heated to an artificial aging temperature 180 ℃ with a commonly used heating rate of 5 ℃/min. SAXS data were collected with a typical data collection time of 30 min for each sample condition during the *in-situ* measurement. Such a data collection time allows reasonable data statistics and time resolution to study the nanostructure and structure evolution of the alloy precipitates. All the SAXS data were normalized to absolute scattering scale, namely, scattering cross section per unit sample volume $I(Q)$ Here, the wave vector transfer $Q = 4\pi\sin(\theta/2)/\lambda$ is defined by the scattering angle θ and the wavelength λ of X-rays.

After 500 min artificial aging for SAXS measurement, the alloy specimen was quickly quenched to room temperature. TEM specimen was prepared by cutting a small piece of sample. TEM observations were conducted using a JOEL 2000FX.

3. Result and discussion

The precipitation sequence of the solution-treated Al-Mg-Si alloys during artificial aging is generally accepted [1-3]: α Super-saturated solid solution (SSS)→ GP-I zones [2] (during the heating process)→ rod-like β" precipitates /or called GP-II zones (transformation from GP-I as nuclei through a diffusion process) → metastable β' precipitates → stable β phase. However, this precipitation sequence does not take into account the natural aging effect. In the present study, we consider the natural aging effect [4,8,9] and introduce a minor route concurrent with the above main route: αSSS→ vacancy-rich clusters (VRC or GP zones, formed during the quenching and the sequent natural aging at RT) → Some clusters will be dissolved during the early stage artificial aging [4], and part of the survived clusters (GP zones) serve as potential nuclei [1,2,4] for transforming into the subsequent β" precipitates. During the artificial aging, the transportation of Mg and Si atoms (from the solid solution to GP-I nuclei and from GP zones to GP-I nuclei) will be much slower due to the consumption of vacancies and solute atoms. This delays, or incubates, the formation or nucleation of β" precipitates.

The time dependent SAXS profiles measured for the naturally aged Al-Mg-Si alloy during the heating process from RT to 180 °C and the subsequent artificial aging at 180 ^{o}C are selectively presented in Fig. 1(a). The standard deviation of the SAXS profiles (RT and 30 min) in Fig. 1(a) is within ±2 %. The SAXS profiles

during the temperature rising process have larger standard deviation with ±25 % due to the unenough counting statistics. The SAXS profiles measured at the temperature rising process and the SAXS profile for the alloy artificially aged at 180 °C for 30 min are nearly the same. In the low-Q region, the power law scattering of Q^{-4} corresponds to the asymptotic scattering behavior of other large particles. The SAXS intensity in the intermediate-Q region measured before 30 min of artificial aging can be attributed to the scattering from the clusters or GP zones formed during the natural aging. The Guinier approximation for the SAXS profile extract a radius of gyration of 2.5 nm for this natural aging clusters. These clusters were also confirmed by our TEM work to the sample before artificial aging although they have not been clearly characterized by other TEM studies yet [1,2]

These steady SAXS profiles observed indicates clearly a short of nanostructural change, *i.e.* no dissolution of the existing clusters and an incubation period of ~30 min since the beginning of artificial aging. The incubation in precipitation can be explained by the significant reduction of the amount of quench-in vacancies and solute atoms (Mg and Si) due to the formation of natural aging clusters. As a consequence, the diffusion of Mg and Si atoms into the precipitates becomes slow during the subsequent artificial aging, thus, the formation of β" precipitates is delayed. The existence of incubation period was roughly shown in a TEM study [4] and SANS study [11], and constantly neglected in the established kinetics [8] and the general knowledge [11] for Al-Mg-Si alloy.

After 30 min aging time, the SAXS profiles in Fig. 1(a) grow with the aging time in the higher Q region ($Q \geq 0.03 Å^{-1}$), indicating a growth of β" precipitates in size and volume fraction as well. Because of the coexistence of natural aging clusters and precipitates due to the concurrent cluster dissolution and precipitation processes, the SAXS profiles measured during the artificial aging at 180°C can be expressed as

$$I(Q) = I_{precip}(Q) + I_{cluster}(Q) = I_{precip}(Q) + \alpha \cdot I_{cluster}(Q, t_0) \qquad (1)$$

where the time-dependent $I_{precip}(Q)$ and $I_{cluster}(Q)$ denote the scattering contributions of the precipitates and the natural aging clusters, respectively. The $I_{cluster}(Q,t)$ can be approximated as the product of the volume fraction of the clusters α and the SAXS profile for the alloy before artificial aging (or the alloy aged at 180℃ for 30 min) $I_{cluster}(Q,t_0)$. The SAXS intensity contributed by the precipitation is thus obtained by the spectra subtraction according to Eq. (1). From a previous experimental evidence [8], the time-dependent volume fraction of the clusters dominates all other cluster effects, such as size, during the dissolution. The SANS study [7] also adopts the spectra subtraction approach to remove the contribution from the other particles.

Theoretically, The α value decreases from unity with increasing the aging time due to dissolution. However, we will assume a time-independent α value in the present study, which will be explained later. If the constant α assumed to be 0, this would mean all the natural aging clusters fully dissolve at the beginning of precipitation, which is not realistic because some clusters survive in fact [1,2,4]. Practically, these original SAXS profiles in Fig. 1a (corresponding to $\alpha = 0$) are difficult to be identified with a typical form factor scattering from monodisperse particles. On the opposite extreme, if we assume that all clusters do not dissolve, *i.e.* α=1.0, the scattering profiles of $I_{precip}(Q)$ obtained from Eq. (1) will exhibit artificial arrows in the lower Q region (Fig. 1(b)) due to the over-subtraction of the cluster contribution. The assumption of α=1.0 is also

not practical because some natural clusters (GP zones) serve as nuclei for transforming into β" precipitates [1,2,4]. From the subtracted SAXS profiles, it can be concluded that $\alpha \neq 0$ and 1.0 during the aging. To avoid the over-subtraction effect for all measured SAXS profiles, an appropriate α value is determined as 0.8, corresponding to the volume fraction of the remaining clusters after the aging. According to the DSC study [8], α value decays to a saturation value after ~ 3hr of aging at 180℃ which implies no dissolution occurs. From our SAXS result and DSC study, it can be assumed the actually time-dependent α value should decay from unity at aging time=0.5hr to a saturation value of ~0.8 after ~ 3hr of aging. Because the analysis result is not sensitive to the variation of α value ranging from 1.0 to 0.8, the α value used in this SAXS analysis (in Eq. (1)) during 0.5hr~3hr can be thus approximated as 0.8, which is the same as the volume fraction of the remaining clusters.

In Fig. 2a, the correctly cluster-subtracted SAXS profiles $I_{precip}(Q)$ (with the deduced α = 0.8) present the temporal evolution of the precipitates during the artificial aging at 180℃. We emphasize that the quality and evolution of the SAXS profiles shown in Figs.1(a) and 2(a) are similar to those of SANS data [10], reflecting the scattering contrast. We model the SAXS intensity of the precipitates of the artificially aged alloy with

$$I_{precip}(Q) = AQ^{-4} + \eta(\Delta\rho)^2 V_P \widetilde{P}(Q) \qquad (2)$$

where the first term, with a constant A, describes the sharp boundary effect of large particles contributing mainly at the lowest-Q region. And the second term denotes the form factor scattering from the rod-like β" precipitates, with the scattering length density difference between precipitates and matrix $\Delta\rho$, the volume fraction η, and the volume V_P of the cylindrical particles of radius R and length L. $\widetilde{P}(Q)$ is the normalized form factor for cylindrical particles [12]. Because the volume fraction of large particles can be assumed not to change all thorough the natural aging and the artificial aging, the coefficient A in Eq. (2) should be fixed in the model analysis. The SAXS background profile (RT and 30 min aging), $I_{cluster}(Q,t_0)$ in Eq. (1), can be expressed as a sum of $B \cdot Q^{-4}$ (B is a constant) and the intensity scattered from the small GP zones. Therefore, a deduced constraint relationship, *i.e.* $A + \alpha \cdot B = B$, should be kept during the model fitting process using Eq. (2).

On the other hand, in the intermediate-Q region, $2\pi / L \leq Q \leq \pi / R$, Eq. (2) can be approximated as $I(Q) \propto \frac{\pi}{Q\ L} \exp(-R^2Q^2/4)$ [13]. This Kratky-Porod approximation implies a linear relationship between $\ln(I(Q)\cdot Q)$ and Q^2 for the rod-like particles in the intermediate-Q region. The radius of rod-like particles can then be conveniently extracted from the slope of the straight line fitted in the $\ln(I(Q)\cdot Q)$ vs. Q^2 plot of the SAXS data. The Kratky-Porod plot is often used to examine the scattering characteristics of rod-like particles and determine model-independently the mean radius R of the rod-like particles. Fig. 2(b) shows the Kratky-Porod approximation (solid lines) in the Q region of 0.03~0.1Å^{-1} for the representative SAXS profiles during the artificial aging. The radii (see Table 1) determined from the slopes of the fitted lines during this aging are nearly the same, indicating a time-independent evolution of the precipitate radius during artificial aging. Furthermore, the SAXS data can also be well fitted using Eq. (2) (selected fitting curves are shown in Fig. 2(a)). And the structural parameters of $\eta(\Delta\rho)^2$, R and L extracted from the model fitting for the precipitates are summarized in Table 1, where we show that the model-fitted radii agree with that obtained by

the model-independent method (Kratky-Porod approximation). The calculated SAXS profiles simulate well the measured SAXS data, as shown in Fig. 2(a).

Several SAS studies [14] on the precipitates of alloys show that the Guinier approximation is still available in the range 0.8<QR<2. In our case, neglecting the small effect of the residual AQ^{-4} contribution, we extract the radius of gyration R_g from the Guinier approximation in the corresponding small Q range around 0.015Å^{-1} to minimize the influence from the large particles. With the values of R and R_g obtained from the Kratky-Porod and Guinier approximations respectively, the length L for the rod-like precipitates can be deduced from $R_g^2 = \frac{L^2}{12} + \frac{R^2}{2}$ [16]. The rod lengths and radii obtained by the model-independent method are listed in Table 1. These values agree with those obtained by the model fitting of Eq. (2). Additionally, the SAXS result of Al-Mg-Si 6022 alloy aged for 500 min is confirmed by the consistent TEM observation of the SAXS specimen, as shown in Fig. 3. Most of the dots in this TEM micrograph are the end-sections of the rod-like β" precipitates oriented along the [100] direction of Al matrix, with an average radius of 2.8±0.6 nm. In a larger sense, SAXS technique, over-sampling a much large number of particles than the TEM technique, can report more faithfully the averaged particle size for precipitates of a significant polydispersity.

In Fig. 4(a), the inert radius and the rapid growing length with the aging time together characterize the structural evolutions of the β" precipitates. These growth characteristics can explain well the transition from spherically nucleated clusters (GP or GP-I zones) to rod-like precipitates, which maintain the same radius of the clusters formed at the beginning of early stage (nucleation) of precipitation. Figure 4(b) shows the two evolutions of relative volume fraction obtained from our SAXS model-fitting result for Al-0.58%Mg-Si alloys and the JMAK kinetics based on the DSC data [8] for Al-0.79%Mg-Si alloys. The present study clearly shows the incubation period and the followed slower diffusion process during the aging of 0~4hr in the precipitation kinetics including the natural aging effect. In principle, precipitation regime enters the coarsening step at 6hr of aging from the coupled nucleation and growth steps, showing the completion of volume fraction development. The temporal evolution of radius and length and volume fraction for the β" precipitates determined by this in-situ SAXS analysis is a new result as the basis of modification of precipitation kinetics.

REFERENCE

[1] Miao WF, Laughlin DE. Scripta Mater 1999; 40:873.

[2] Edwards G.A, Stiller K, Dunlop GL, Couper MJ. Acta Mater 1998; 46:3893.

[3] Marioara CD, Andersen SJ, Jansen J, Zandbergen HW. Acta Mater 2001; 49:321.

[4] Marioara CD, Andersen SJ, Jansen J, Zandbergen HW. Acta Mater 2003; 51:789.

[5] Perovic A, Perovic DD, Weatherly G.C, Lloyd DJ. Scripta Mater 1999; 41:703.

[6] Esmaeili S, Wang X, Lloyd DJ, Poole WJ. Metall Trans A 2003; 34:751.

[7] Donnadieu P, Carsughi F, Redjaïmia A, Diot C, Lapasset GJ. Appl Crystallogr 1998; 31:212.

[8] Esmaeili S, Lloyd DJ, Poole WJ. Acta Mater 2003; 51:3467.

[9] Poole WJ, Lloyd DJ, Embury JD. Mater Sci Eng A 1997; 234-236:306.

[10] Schiffmann R, Haug J, Banhart J. Proceedings of 9th International Conference on Aluminum Alloys. 2004; p. 604.

[11] Myhr OR, Grong Ø. Acta Mater 2000; 48:1605.

[12] Guinier A, Fournet G.. *Small Angle X Ray Scattering*. New York: John Wiley; 1955.

[13] Glatter O, Kratky O. *Small Angle X Ray Scattering*. New York: Academic Press; 1982.

[14] Werenskiold JC, Deschamps A, Bréchet Y. Mater Sci Eng A 2000; 293:267.

Table 1. Comparison of the structural parameters determined by the model fitting and model-independent methods.

Aging time (min)	R^a (nm)	L^a (nm)	R^b (nm)	R_g (nm)	L^c
60	2.70	6.0	2.82	3.24	8.85
90	2.62	12.1	2.43	3.87	12.01
130	2.75	13.1	2.43	4.06	12.74
160	2.81	14.5	2.94	4.26	12.88
220	2.71	15.2	2.59	4.33	13.59
300	2.85	16.6	2.70	4.48	14.00
430	2.88	16.5	2.76	4.51	14.08
500	2.82	16.9	2.93	4.51	13.90

[a] Parameters for the radius *R* and length *L* determined from the model-fitting.

[b] Rod radius obtained independently by the Kratky-Porod approximation.

[c] Rod length determined using $R_g^2 = \frac{L^2}{12} + \frac{R^2}{2}$ together with the radii obtained from the Guinier and Kratky-Porod approximations.

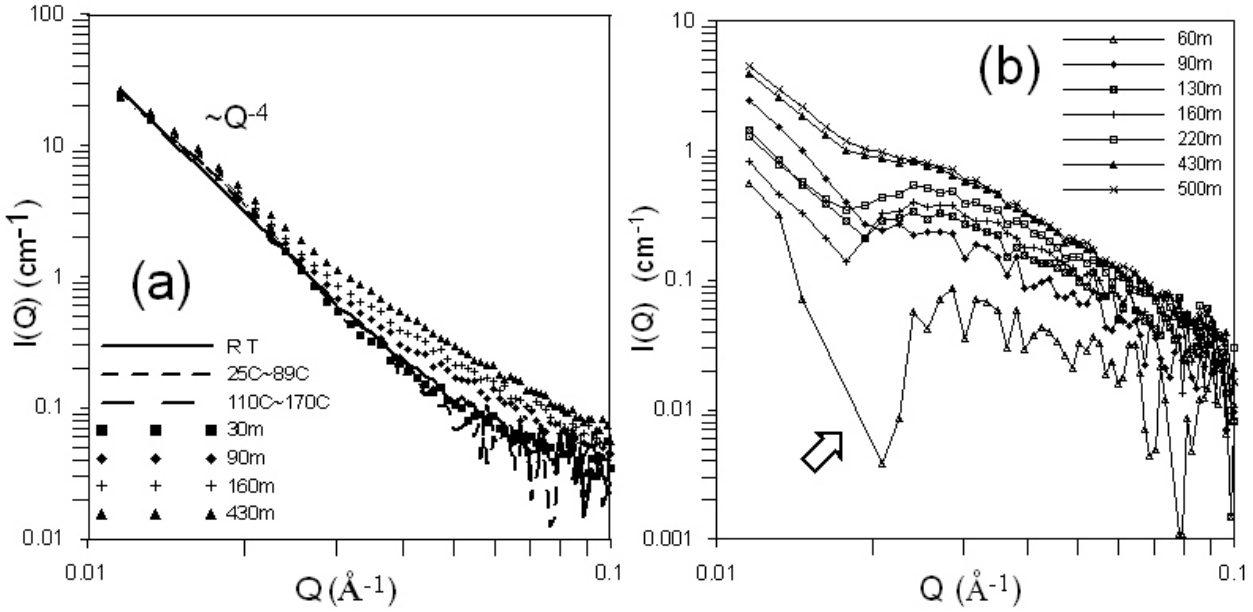

Fig. 1(a) Time-dependent SAXS profiles for the naturally aged Al-Mg-Si alloy during the heating and the subsequent isothermally artificial aging at 180°C (selectively presented). (b) The measured SAXS profiles are subtracted with the SAXS profile for 30 min aging for removing the cluster contribution (assuming $\alpha = 1.0$). The arrow shows the dips due to the over-subtraction effect.

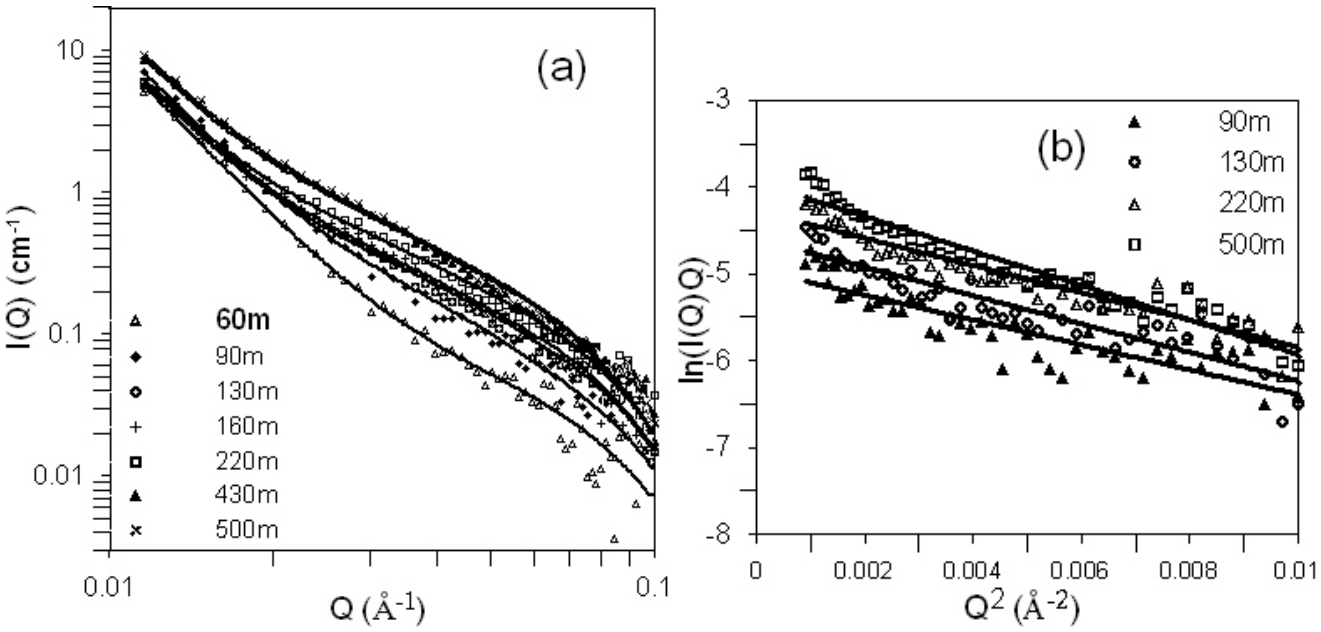

Fig. 2(a) The correctly cluster-subtracted SAXS profiles as those in Fig. 1(b) but corrected with a deduced α value of 0.8. The SAXS profiles are fitted (solid lines) using a rod-like model for the structural evolution of precipitates of the Al-Mg-Si alloy aged at 180 °C with aging time. (b) The selected SAXS profiles from (a) are fitted (solid lines) using the Kratky-Porod approximation for the temporal evolution of radius of the precipitates (Note, part of the low-Q data are omitted for clarity).

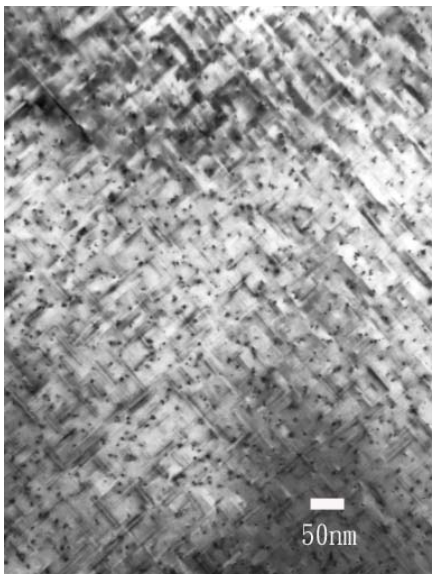

Fig. 3 TEM micrograph ($[100]_{Al}$ zone axis)

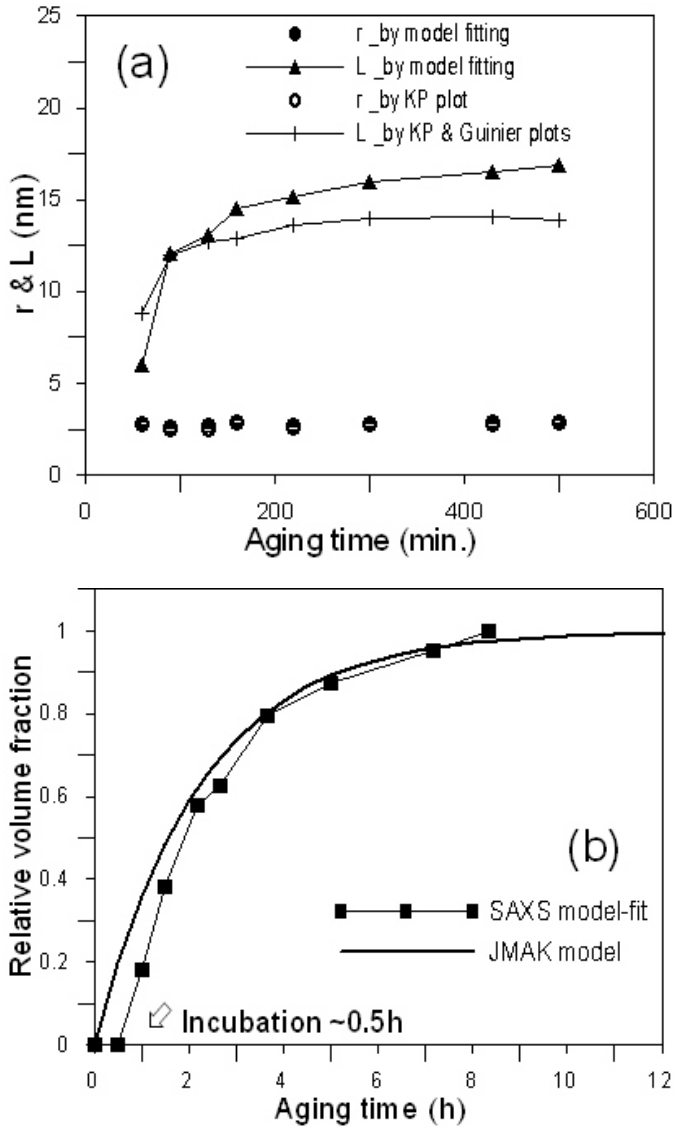

Fig. 4 (a) The structural evolution of the β" precipitates with aging time. The length L and radius r of the rod-like precipitates are extracted from the SAXS data in Fig. 2. (b) The temporal evolution of the relative volume fraction of precipitates deduced from the SAXS data and DSC result (based on the JMAK model).